Journal of Applied Mechanics and Technical Physics, Vol. 49, No. 5, pp. 799–808, 2008

OIL LOW TO A LATERAL WELL IN THE PRESENCE OF BOTTOM WATER

Yu. I. Kapranov and V. N. Émikh

UDC 532.546.06

Exact solutions are obtained for a number of two-dimensional problems of steady-state fluid flow to a lateral hole in a reservoir with a quiescent bottom fluid of higher density or with a fluid of lower density at the reservoir top.

Key words: *lateral well, filtration velocity hodograph, mapping parameters, interface, critical flow regime.*

Introduction. In oil production practice, one often encounters situations in which the flow domain can be divided with sufficient accuracy into several parts separated from each other by boundaries which are not known beforehand. The fluid moving in each of the indicated subdomains differs in properties from the fluids in the neighboring subdomains [1, 2]. One of the best-known problems related to flows of this type is the problem of the so-called bottom water coning [2–4]. Approaches to constructing solutions for such problems, which are mostly of approximate nature, have been developed most fully for straight holes. From a practical point of view, the main goal of these approaches is to determine conditions under which bottom water breakthrough into a producing well is impossible.

In recent decades, considerable attention has been paid to similar problems for the case of lateral holes, which have a number of advantages over straight holes. In particular, being located along beddings, they have a considerably larger are of contact with the oil pool, which provides much higher production rates. However, for the same reason, in the case of bottom water through into a lateral hole, the rate of water encroachment is much higher than that in the case of a straight hole. In view of the aforesaid, of particular importance are studies aimed at finding the class of flows that are critical for water-free oil production.

Strictly speaking, such regimes can be analyzed only on the basis of exact solutions of the corresponding problems. However, because the latter are difficult to solve, such solutions are few in number not only for unsteady but also for steady-state problems. A simple analytical solution for the critical flow regime in an homogeneous, infinitely thin inclined layer of infinite length was first obtained in [5] where a linear periodic chain of wells was modeled by point drains. Among the advantages of the cited study is the simplicity of the solution constructed. The present paper also deals with constructing exact solutions for the case of horizontal wells but, unlike in [5], the formulation adopted here is more realistic.

1. Formulation of the Problem and Parametric Representation of the Solution. A general flow diagram is presented in Fig. 1. The motion is considered steady-state and two-dimensional in the vertical plane xOy, and the axis Ox is horizontal. It is assumed that the reservoir of thickness T is homogeneous and has finite length and the bottom $y = 0$ of the reservoir and its top $y = T$ are impermeable. At a distance H from the top there is a producing lateral well, whose axis is perpendicular to the plane xOy. The well operates at a constant capacity $2Q$ per its unit length. In the flow plane, it is modeled by a point A.

We consider flow of a fluid of density ρ_1 and viscosity μ_1 which moves from infinity to the well and is symmetric about the Oy axis. At the bottom of the reservoir, separated from the main part of the flow by the interface BC, there is a quiescent fluid of density $\rho_2 > \rho_1$ and viscosity μ_2, which generally does not coincide with μ_1. The adopted model can be interpreted not only as oil pumping from a reservoir with underlying bottom

Lavrent'ev Institute of Hydrodynamics, Siberian Division, Russian Academy of Sciences, Novosibirsk 630090; emikh@hydro.nsc.ru. Translated from Prikladnaya Mekhanika i Tekhnicheskaya Fizika, Vol. 49, No. 5, pp. 114–126, September–October, 2008. Original article submitted June 29, 2007.

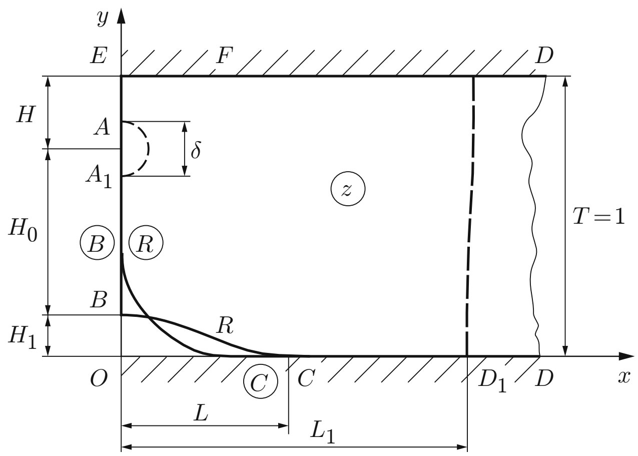

Fig. 1. Flow domain in a reservoir with a bottom fluid.

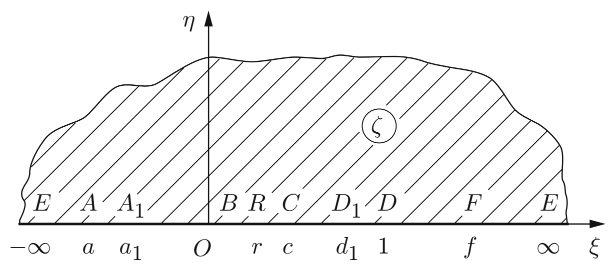

Fig. 2

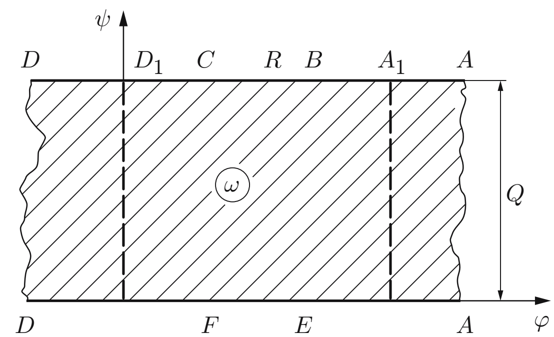

Fig. 3

Fig. 2. Half-axis of the auxiliary complex variable.

Fig. 3. Domain of the complex potential.

water, but also, for example, as flow to a well in a water-bearing reservoir containing a heavier contaminated fluid. With any of these interpretations, the primary goal is to calculate the reservoir production conditions that rule out bottom fluid breakthrough into the well. Figure 1 shows the right half of the flow domain studied.

The corresponding boundary-value problem consists of finding the complex flow potential $\omega = \varphi + i\psi$ as an analytical function of the coordinates $z = x + iy$ of the points of the filtration region under the following boundary conditions:

$$\begin{gathered} AE\colon\quad x = 0,\quad \psi = 0; \qquad AB\colon\quad x = 0,\quad \psi = Q; \qquad ED\colon\quad y = 1,\quad \psi = 0; \\ CD\colon\quad y = 0,\quad \psi = Q; \qquad BC\colon\quad \varphi - \rho y = \text{const},\quad \psi = Q \quad [\rho = (\rho_2 - \rho_1)/\rho_1]. \end{gathered} \tag{1}$$

Here and below, use is made of the functions ω and z normalized by the quantities $\varkappa_1 T$ and T ($\varkappa_1$ is the filtration coefficient of the moving fluid). The first condition in the domain BC is a consequence of the assumption of motionless bottom water and the dynamic condition of pressure continuity in passing through the oil–water interface [1–3].

For a parametric representation of the solution, the domain of the complex potential ω (Fig. 3) and the domain of the function $1/w$ (Fig. 4) performing inversion of the filtration velocity hodograph $\bar{w} = w_x + iw_y$ (Fig. 5) with respect to a unit circle with center at the coordinate origin are mapped onto the half-plane $\operatorname{Im}\zeta \geqslant 0$ (Fig. 2). The maps can be represented as

$$\omega = \omega_C - \frac{Q(1-a)}{\pi} \int\limits_c^\zeta \frac{d\zeta}{(\zeta - a)(1-\zeta)} = \omega_C - \frac{Q}{\pi} \ln \frac{(\zeta - a)(1-c)}{(1-\zeta)(c-a)}; \tag{2}$$

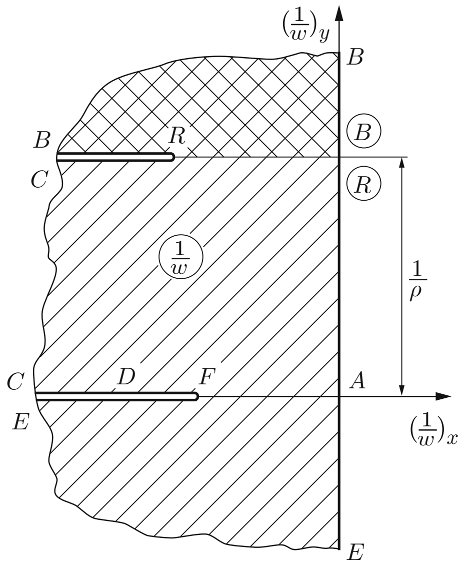

Fig. 4

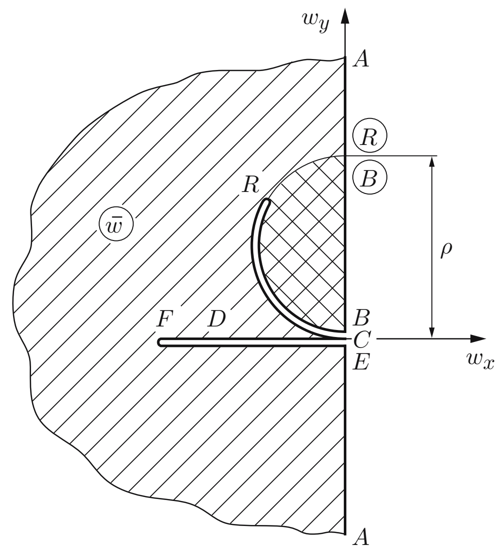

Fig. 5

Fig. 4. Domain of inversion of the velocity hodograph.

Fig. 5. Domain of the velocity hodograph.

$$\frac{1}{w} = \frac{dz}{d\omega} = iM\int\limits_a^\zeta \frac{(f-\zeta)(r-\zeta)\,d\zeta}{(c-\zeta)(-\zeta)\sqrt{-\zeta}} = 2iM\Big\{Z\Big[1+\frac{fr}{c\sqrt{a\zeta}}\Big] + \sigma[G(\zeta)-G]\Big\}$$
$$(-\infty < \zeta \leqslant 0), \tag{3}$$

where

$$Z = \sqrt{-a} - \sqrt{-\zeta}, \quad G(\zeta) = \arctan\sqrt{-c/\zeta}, \quad G = G(a), \quad \sigma = (f-c)(c-r)/\sqrt{c^3}. \tag{4}$$

The main problem is to find the parameters a, c, f, r, and M included in representations (2)–(4). To determine the quantity ω_C contained in dependence (2), one needs to specify the value ω at a certain point of the reservoir, which will be required in Sec. 4 for a different formulation of the problem. In the adopted formulation with the well capacity specified, in which the pressure can be determined only to within an arbitrary constant, such detailing is not necessary.

2. Critical Flow Regime. As a first step, we study restrictions on the parameter Q that rule out bottom water breakthrough into the well. We consider the case $r = 0$. In this case, the domain ω and their corresponding dependence (2) are preserved, and in the domain $\bar{w}$, the vertex R of the arc cut reaches the w_y axis and coincides with the point B. As a result, the half-circle $\{|w - i\rho/2| \leqslant \rho/2,\ w_y \leqslant 0\}$ falls out of the hodograph, and the quadrant $\{\mathrm{Im}\,(1/w) \geqslant 1/\rho, \mathrm{Re}\,(1/w) \leqslant 0\}$ falls out of the domain of inversion of the hodograph. In Figs. 4 and 5, the indicated subdomains are shaded in two directions. The points B and R, corresponding to this limiting case and the point C in Fig. 1 are enclosed in circles.

The relation

$$p = -\rho_1 g(\varphi + y) \tag{5}$$

implies the inequality $dp/dy = -\rho_1 g(w_y + 1) \leqslant -\rho_2 g$, which is satisfied on the segment AB. In this case, the equality characterizing the hydrostatic equilibrium of the underlying fluid is preserved only at the point B, and at the points of the segment AB, the hydrodynamic pressure gradient exceeds the stabilizing effect of gravity on bottom water, and a further arbitrary small pressure decline should entrain it in the flow. Thus, in the critical regime, the maximum admissible wells capacity is determined.

According to the above-mentioned changes in the hodograph inversion domain, dependence (3) for the boundary segment EAB becomes

$$\frac{1}{w} = 2iM[\tau(-a) - \tau(-\zeta)], \qquad \tau(t) = \frac{f-c}{\sqrt{c}} \arctan\sqrt{\frac{t}{c}} + \sqrt{t}. \tag{6}$$

For $\zeta = 0$ and $w = -i\rho$, this leads to

$$2\rho M\tau(-a) = 1. \tag{7}$$

On the segment BC ($0 \leqslant \zeta \leqslant c$), in view of (6), we have

$$\frac{1}{w} = i\,\frac{1}{\rho} - M\int\limits_0^\zeta \frac{(f-\zeta)\,d\zeta}{(c-\zeta)\sqrt{\zeta}}.$$

Comparing the increments of both sides of the last equality in circulation about the point C (see Fig. 4), we obtain

$$M = \sqrt{c}/[\pi\rho(f-c)]. \tag{8}$$

Substituting this expression instead of M into (7) and using representations (4) and (6) for G and $\tau(t)$, respectively, we obtain the relation

$$\sqrt{-ac}/(f-c) = G.$$

In view of equality (8), the parameters M and f can be expressed in terms of a and c:

$$M = G/(\pi\rho\sqrt{-a}), \qquad f = c + \sqrt{-ac}/G. \tag{9}$$

Using (9), we represent relation (6) as

$$\frac{1}{w} = i\,\frac{2}{\pi\rho}\Big(G(\zeta) - \sqrt{\frac{\zeta}{a}}\,G\Big) \qquad (-\infty < \zeta \leqslant 0). \tag{10}$$

On the other two segments of the real axis of the plane ζ, the indicated relation is rearranged as follows:

$$\frac{1}{w} = -\frac{1}{\pi\rho}\Big(\Lambda(\zeta) + 2\sqrt{-\frac{\zeta}{a}}\,G\Big) + i\,\frac{1}{\rho} \qquad (0 \leqslant \zeta \leqslant c); \tag{11}$$

$$\frac{1}{w} = -\frac{1}{\pi\rho}\Big(\Lambda(\zeta) + 2\sqrt{-\frac{\zeta}{a}}\,G\Big), \qquad \Lambda(\zeta) = \ln\Big|\frac{\sqrt{\zeta}+\sqrt{c}}{\sqrt{\zeta}-\sqrt{c}}\Big| \quad (c \leqslant \zeta < \infty). \tag{12}$$

According to (3), the equality $dy/dx = \operatorname{Im}(1/w)/\operatorname{Re}(1/w)$ holds at each point of the flow domain. In view of (11), this leads to $\lim\limits_{\zeta\to+0}(dy/dx) = -\infty$. Thus, in the limiting case considered, the point B is an apex of the interface BC.

Setting $\zeta = 1$ and $w = -Q$ in equality (12), we obtain the equation

$$\Pi - 2G/\sqrt{-a} = 0, \tag{13}$$

where

$$\Pi = \frac{\pi\rho}{Q} - \ln\frac{1+\sqrt{c}}{1-\sqrt{c}}. \tag{14}$$

Equation (13) uniquely defines the dependence $c = c(a)$ at each point of the half-axis $a < 0$; $c \in (0,1)$.

The physical parameters to be specified include the depth H (reckoned from the top of the reservoir) of the point drain A which models the well (see Fig. 1). Using the first equality in (3) and relations (2) and (10), for the quantity H we obtain the representation

$$H = \frac{2Q(1-a)}{\pi^2\rho}\int\limits_{-\infty}^{a} \frac{\sqrt{\zeta/a}\,G - G(\zeta)}{(a-\zeta)(1-\zeta)}\,d\zeta, \tag{15}$$

which is used to find the parameter a. In this case, the right side of (15) is treated as a complex function $F(a)$ of the parameter a, i.e., as c it uses the dependence $c = c(a)$ determined from (13). Numerical calculations show that

TABLE 1

H	V						
	$q = 0.2$	$q = 0.5$	$q = 1$	$q = 5$	$q = 10$	$q = 50$	$q = 100$
0	0.8047	0.2788	0.1021	0.0052	0.0013	$52 \cdot 10^{-6}$	$13 \cdot 10^{-6}$
0.1	0.7582	0.2629	0.0967	0.0049	0.0012	$50 \cdot 10^{-6}$	$12 \cdot 10^{-6}$
0.2	0.6523	0.2229	0.0823	0.0042	0.0011	$43 \cdot 10^{-6}$	$12 \cdot 11^{-6}$
0.3	0.5188	0.1716	0.0630	0.0033	$82 \cdot 10^{-5}$	$33 \cdot 10^{-6}$	$82 \cdot 10^{-7}$
0.4	0.3776	0.1193	0.0431	0.0022	$56 \cdot 10^{-5}$	$22 \cdot 10^{-6}$	$56 \cdot 10^{-7}$
0.5	0.2447	0.0731	0.0257	0.0013	$33 \cdot 10^{-5}$	$13 \cdot 10^{-6}$	$33 \cdot 10^{-7}$
0.6	0.1337	0.0377	0.0128	$62 \cdot 10^{-5}$	$16 \cdot 10^{-5}$	$62 \cdot 10^{-7}$	$16 \cdot 10^{-7}$
0.7	0.0559	0.0150	0.0048	$22 \cdot 10^{-5}$	$56 \cdot 10^{-6}$	$22 \cdot 10^{-7}$	$56 \cdot 10^{-8}$
0.8	0.0148	0.0037	0.0011	$48 \cdot 10^{-6}$	$12 \cdot 10^{-6}$	$48 \cdot 10^{-8}$	$12 \cdot 10^{-8}$
0.9	0.0014	$29 \cdot 10^{-5}$	$77 \cdot 10^{-6}$	$31 \cdot 10^{-7}$	$78 \cdot 10^{-8}$	$31 \cdot 10^{-9}$	$78 \cdot 10^{-10}$

the function $F(a)$ increases monotonically from 0 to 1 as the parameter a varies from $-\infty$ to 0. By virtue of this, the parameters a and c are uniquely determined in their intervals of variation for any value of $H \in (0,1)$. After that, the parameters M and f are calculated from formulas (9).

After finding all mapping parameters, we determine the distance H_0 from the drain A to the apex B of the bottom water cone (see Fig. 1). The expression for this quantity is also found taking into account relation (10) [compare with (15)]:

$$H_0 = \frac{2Q(1-a)}{\pi^2 \rho} \int\limits_a^0 \frac{G(\zeta) - \sqrt{\zeta/a}\, G}{(\zeta - a)(1-\zeta)}\, d\zeta.$$

Integration of the first equality in (3) with the use of relations (2) and (11) yields the complex-parametric equation for the interface BC between oil and water:

$$x + iy = \frac{Q(1-a)}{\pi^2 \rho} \int\limits_0^\zeta \frac{\Lambda(\zeta) + 2\sqrt{-\zeta/a}\, G}{(\zeta - a)(1-\zeta)}\, d\zeta + i\Big(H_1 - \frac{Q}{\pi\rho}\, N(\zeta)\Big),$$
$$N(\zeta) = \ln \frac{\zeta - a}{(1-\zeta)(-a)}. \tag{16}$$

Setting $\zeta = c$, $x = L$, and $y = 0$, we obtain formulas for the width L and height H_1 of the bottom water crest:

$$L = \frac{Q(1-a)}{\pi^2 \rho} \int\limits_0^c \frac{\Lambda(\zeta) + 2\sqrt{-\zeta/a}\, G}{(\zeta - a)(1-\zeta)}\, d\zeta, \qquad H_1 = \frac{Q}{\pi\rho} N \quad (N = N(c)).$$

The quantities H, H_0, and H_1 are linked by the relation $H + H_0 + H_1 = 1$, which can be used as a control one or to find one of the two quantities H_0 and H_1 if the other is known.

One of the basic flow characteristics calculated for the critical regime is the maximum volume V of bottom water that remains motionless for the given well capacity Q:

$$V = \int\limits_0^c y\Big(\frac{dx}{d\zeta}\Big)\, d\zeta. \tag{17}$$

The coordinates x and y of the interface BC contained in the right side of this expression are determined in (16).

The dependence on the quantities Q and ρ in Eqs. (13) and (15) and in all relations obtained on the basis of the representation for z is expressed only in terms of the relation $q = Q/\rho$. This implies that the mapping parameters and geometrical flow characteristics (including V) are invariant under a proportional change in Q and ρ. Table 1 gives values of V calculated for various values of H and q for the limiting case considered. From the table it follows that, for small values of the quantity V, it is inversely proportional to q^2. In view of the dependences for $1/w$, the aforesaid implies that, with proportional changes in the quantities Q and ρ, the filtration velocity components at each point of the flow also change proportionally.

Below, the subscript asterisk denotes the filtration characteristics and the mapping parameters calculated for the critical regime if their values generally differ from the limiting ones.

In practice, the critical pumping regime can be identified by increasing the well capacity until bottom water begins to invade the well. The initially unknown volume V of bottom water is calculated from formula (17) and is then used as one of the parameters determining the flow characteristics in the normal regime, where $Q < Q_*$.

3. General Case. Relations (2) and (3), used in the solution of the boundary-value problem, generally contain five unknown parameters: M, a, c, f, and r. As for the critical regime, the algorithm for finding these parameters ultimately reduces to solving the system of equations for the parameters a and c, in terms of which the parameters M, f, and r should first be expressed.

On the segment BC $(0 \leqslant \zeta \leqslant c)$, equality (3) is represented as

$$\frac{1}{w} = -M\Big(2\,\frac{\Phi(\zeta)}{\sqrt{\zeta}} + \sigma\Lambda(\zeta)\Big) - 2iM\Big(\frac{ac + fr}{c\sqrt{-a}} - \sigma\arctan\sqrt{-\frac{a}{c}}\,\Big), \quad \Phi(\zeta) = \zeta + \frac{fr}{c}, \tag{18}$$

where the function $\Lambda(\zeta)$ is defined in (12). Comparing the increments of both sides of equality (18) in circulation about the point C and using expressions (4) for σ, we obtain

$$M = \frac{1}{\pi\rho}\,\frac{\sqrt{c^3}}{(f - c)(c - r)}. \tag{19}$$

Since $\mathrm{Im}\,(1/w) = 1/\rho$ on BC, by virtue of (18) and (19), we have

$$\frac{-ac - fr}{(f - c)(c - r)} = \sqrt{-\frac{a}{c}}\,G. \tag{20}$$

On the segment CE $(c \leqslant \zeta < \infty)$, the dependence for $1/w$ becomes

$$\frac{1}{w} = -2M\Big(\sqrt{\zeta} + \frac{fr}{c\sqrt{\zeta}}\Big) - \frac{1}{\pi\rho}\,\Lambda(\zeta).$$

Setting $\zeta = 1$ and $w = -Q$ and using (19) and (20), from this we obtain

$$\Pi - \frac{2\sqrt{c}\,(c + fr)}{(f - c)(c - r)} = 0, \tag{21}$$

where the function Π is defined in (14). Eliminating the parameter f from equality (21) in view of (20), we have the equation

$$\begin{gathered} Ar^2 + Br + C = 0, \\ B = 2(1 - c)\sqrt{-a}\,G - (c - a)\Pi - 2(1 - a)\sqrt{c}, \\ A = 2\sqrt{-a}\,G + \Pi, \qquad C = -ac(\Pi - 2G/\sqrt{-a}\,). \end{gathered} \tag{22}$$

Because the interchange of the parameters f and r does not change the dependences leading to Eq. (22), by eliminating the parameter r from (21), we obtain an equation for f similar to (22), which has the following roots:

$$r_{1,2} = -B \pm \sqrt{\Delta} \qquad (\Delta = B^2 - 4AC). \tag{23}$$

From equality (21), it follows that $\Pi > 0$. In view of this and using the estimate $G < \sqrt{-c/a}$, we have

$$B < 0, \qquad \Delta > 0.$$

From this, we conclude that roots (23) of Eqs. (22) are real. The smaller root r_2 is contained in the interval $(0, c)$, thus determining the parameter r (see Fig. 5), and the larger root satisfies the inequality $r_1 > c$ and determines the parameter f. Because the roots of Eq. (22) are positive for the examined flow model, the condition $C > 0$ should be satisfied, i.e.,

$$F(a, c) = \Pi - 2G/\sqrt{-a} > 0. \tag{24}$$

By virtue of Eqs. (19), (20), and (22), finding the unknown mapping parameters reduces to determining the parameters a and c for the same quantities H and V as in the limiting case.

Integration of (3) with the use of (2) yields

$$H = \frac{2Q(1-a)}{\pi^2\rho} \int\limits_{-\infty}^{a} \frac{[G - G(\zeta)] - \pi\rho M Z[1 + fr/(c\sqrt{a\zeta}\,)]}{(a-\zeta)(1-\zeta)}\, d\zeta. \tag{25}$$

Using relations (2), (3), and (17), we obtain the parametric representation of the interface BC

$$x + iy = \frac{Q(1-a)}{\pi^2\rho} \int\limits_{0}^{\zeta} \frac{2\pi\rho M\Phi(\zeta) + \Lambda(\zeta)\sqrt{\zeta}}{(\zeta - a)(1-\zeta)\sqrt{\zeta}}\, d\zeta + i\Big(H_1 - \frac{Q}{\pi\rho}\, N(\zeta)\Big). \tag{26}$$

The function $N(\zeta)$ included in this representation is defined in (14).

According to (17) and (26), the quantity V is given by the equality

$$V = H_1 L - \frac{Q^2(1-a)}{\pi^3\rho^2} \int\limits_{0}^{c} \frac{2\pi\rho M\Phi(\zeta) + \Lambda(\zeta)\sqrt{\zeta}}{(\zeta - a)(1-\zeta)\sqrt{\zeta}}\, N(\zeta)\, d\zeta. \tag{27}$$

The quantities L and H_1 are calculated using (26) for $\zeta = c$.

The parameters a and c from Eqs. (25) and (27) are calculated using nested iterations. The right side of Eq. (27) is treated as a complex function of the parameter c. This implies that, for each value of c fixed during the solution of the equation, the parameter a is determined from Eq. (25). It is established numerically that the right side of Eq. (25) increases monotonically from zero to a certain value of $H_* > H$ as the parameter a increases from $-\infty$ to a_*, and the right side of Eq. (27) increases from zero to $V_* > V$ as the parameter c increases from zero to the values c_*, which, similarly to the value a_*, is calculated previously for the limiting flow regime with a chosen value $Q < Q_*$. The aforesaid provides unique solvability of the iterative procedure described above; in this case,

$$a \in (-\infty,\ a_*), \qquad c \in (0,\ c_*). \tag{28}$$

From a physical point of view, the inequality $V_* > V$ implies that smaller well capacities correspond to larger values of the maximum volume V_* of bottom water that remains in the state of rest.

Reverting to inequality (24), we note that the function $F(a, c)$ contained in it increases monotonically with decreases in each of the parameters a and c. In view of (13), from this it follows that, under restrictions (28), inequality (24) is satisfied. During the solution of system (25), (27), we also calculate the parameters f, r, and M included in them. Using relations (22) and (23), it is possible to show that, in the limiting case, for $r_2 = C = 0$, the root $r_1 = -B/A$ is defined by the same expression as the parameter f in (9).

From relations (2) and (3), the quantity H_0 is expressed as

$$H_0 = \frac{2Q(1-a)}{\pi^2\rho} \int\limits_{a}^{0} \frac{[G(\zeta) - G] + \pi\rho M Z[1 + fr/(c\sqrt{a\zeta}\,)]}{(\zeta - a)(1-\zeta)}\, d\zeta.$$

The calculations can generally be checked using the relation $H + H_0 + H_1 = 1$.

4. Modification of the Initial Formulation of the Problem. Let us assume that, at identical distances from the well on both sides of it, there are external reservoir boundaries with specified pressure heads; in this case, the flow symmetry about the plane $x = 0$ of the initial formulation of the problem is preserved. The flow domain also includes the internal equipotential that has a common point A_1 with the well contour; the pressure p_1 at this point should be specified. The boundary equipotentials of the filtration region are denoted in Figs. 1 and 3 by dashed curves.

The wellbore pressure p_0 can be measured directly in the well. It is linked to the quantity p_1 by the relation $\Delta p = p_1 - p_0$, where Δp characterizes the pressure losses during fluid passage through the well filter. The quantity Q is to be determined.

In the formulation considered (unlike in the initial one), one should previously determine the constant ω_C in representation (2) for the potential ω, which is linked to the pressure by relation (5). For this, we use the condition

$$p_{D_1} = \varphi_{D_1} = 0. \tag{29}$$

According to (29), the lower point D_1 of the external boundary is taken to be the reference point for the pressure and potential; in this case, in the flow domain, $p < 0$ and $\varphi > 0$.

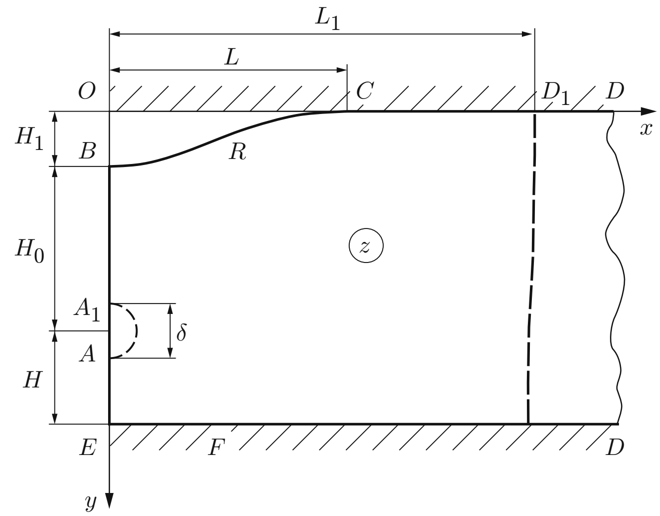

Fig. 6. Flow domain in a reservoir with a fluid under the top of the reservoir.

The basis of the computational algorithm is the finding of the capacity $Q \in (0, Q_*)$ at $p_1 = p_0 + \Delta p$, where $p_0 \in (0, p_{0*})$ is the specified well pressure. Ultimately, this procedure reduces to numerical solution of the equation

$$p_1^0 = \frac{p_1}{\rho_1 g} = -\varphi_1 - H_0 - H_1 + \frac{\delta}{2}, \qquad \varphi_1 = \varphi_{A_1} = \frac{Q}{\pi} \ln \frac{(d_1 - a)(1 - a_1)}{(a_1 - a)(1 - d_1)}. \tag{30}$$

Here d_1 and a_1 are the affixes of the points D_1 and A_1, respectively, calculated from the specified coordinates $x_{D_1} = L_1$ and $y_{A_1} = H_0 + H_1 - \delta/2$ on the interface. The expression for the quantity φ_1 in (30), which is equal to the potential difference across the well and the external boundary, is obtained from relations (2), in which the constant φ_C is determined on the basis of (29).

For each value of Q, fixed during the solution of Eq. (30), the parameters M, a, c, f, and r are calculated using the algorithm described in Sec. 3. The implementation of this algorithm involves restrictions (28), the second of which allows one to obtain the parameter r as one of the roots of Eq. (22). According to this, the sequence of solution of subsystem (25), (27) changes: the left side of Eq. (25) is treated as a complex function of the parameter $a \in (-\infty, 0)$, and the parameter c is determined in the internal cycle of the iterative procedure by solving Eq. (27). In each step of the cycle, the upper bound c_* of the admissible values of the parameter c dependent on the parameters a and Q is calculated previously from relation (13). Equation (30) is solved assuming that the function $p(Q)$ increases monotonically for $Q \in (0, Q_*)$. This fact was established numerically.

5. Case of a Quiescent Fluid of Lower Density at the Reservoir Top. We assume that, above a fluid flow of density ρ_2 and viscosity μ_2 there is a fluid of density ρ_1. The latter has viscosity μ_1, which, generally speaking, differs from μ_2 and is adjacent to the top of the reservoir. In this case, the domain z presented in Fig. 6 is a specular reflection of the initial filtration region in the x axis. In the boundary-value problem, boundary conditions (1) are preserved, including the first condition on BC, in which the parameter ρ is given by the equality

$$\rho = (\rho_2 - \rho_1)/\rho_2. \tag{31}$$

For $\rho_1 = 0$ and $\rho = 1$, equality (31) becomes the well-known condition on the free surface, and the boundary-value problem describes filtration to a well in a gas-capped oil reservoir.

The domains of the remaining functions used in the solution of the problem, are symmetric, as in the domain z, to the corresponding domains presented In Figs. 2–5 about the abscissa. This implies that all the analytical dependences obtained above are extended to the flow considered. Nevertheless, for the same determining physical parameters, the corresponding filtration characteristics are different since, for the same densities ρ_1 and ρ_2, the parameter ρ of the initial flow model and the one considered here has different values.

The maximum volume of the fluid which is quiescent above the flow for the specified well capacity is determined, as before, for the critical regime in which the point B becomes the apex of the line of intersection. In this case, $p = -\rho_2 g(\varphi - y)$, and the relation $w_y = d\varphi/dy \geqslant \rho$ for the parameter ρ defined according to (31) leads to the inequality $dp/dy = -\rho_2 g(w_y - 1) \leqslant -\rho_1 g$. Thus, in the case considered, the critical flow regime also occurs on the verge of violation of the hydrostatic equilibrium of the quiescent fluid.

6. Numerical Calculations and Flow Analysis. The analytical dependences obtained were used to develop algorithms for calculating flow characteristics. In each of the two formulations of the boundary-value problem considered above, the determining physical parameters are the densities of the filtering and quiescent fluids and the distance from the reservoir top to the point drain A modeling the well, and if the well pressure is specified, the determining parameters include the well diameter (in this case, the flow model includes the external boundary).

As regards the well capacity or the well pressure, before specifying any of these parameters, one should find its maximum admissible value in the critical regime and the volume V of the fluid that remains motionless during well pumping (this quantity is included in the number of determining physical parameters during subsequent calculations for the normal flow regime).

Let us consider an example of calculations using the computational procedure described above for a particular combination of input parameters, assuming $\rho_1 = 0.8$, $\rho_2 = 1$, and $H = 0.2$ and specifying the pressure in a well of diameter $\delta = 0.01$ and the abscissa $L_1 = 3$ of the point D_1 of the external boundary. The superscript 0 of the piezometric height $p^0 = p/(\rho_1 g)$ used in the calculations is omitted.

Let us assume that a lighter fluid is filtered. In this case, according to (1), we have $\rho = 0.25$. For the critical regime, we set $Q = Q_* = 1$ and $p_0 = p_{0*} = -6$; hence, $V = 0.006\,55$, $H_1 = 0.1729$, $L = 0.1131$, and $p_{1*} = -5.0624$. Thus, the value $\Delta p = 0.9376$ is set equal to the pressure losses during fluid passage through the filter. Using this parameter to correct the quantity p_0, in the further calculations, we can assume that the pressure p_1 is specified at the point A_1 on the well. In each calculation, the parameters determining the flow include the volume V of bottom water found from Eq. (27) for the critical regime.

For $p_1 = -4$, -2, -1, -0.8, and -0.7971, we obtain $Q = 0.7510$, 0.2824, 0.0480, 0.0012, and 0.0005, $H_1 = 0.0981$, 0.0535, 0.0260, 0.0063, and 0.0044, and $L = 0.1322$, 0.2020, 0.3933, 1.7526, and 2.6338. According to (30), for $p_1 = -0.8$ and -0.7971, the potential difference across the well and the external boundary decreases to values $\varphi_1 = 0.0050$ and 0.0021 respectively, resulting in almost complete cessation of the fluid influx into the well and water spread over the reservoir bottom.

The well depth and the specified well pressure (or capacity) are technological parameters that determine the pumping conditions. In a particular situation, they should be matched to the native state reservoir characteristics. These parameters include the quantities V and ρ, and in the formulation with specified well pressure, they also include the reservoir pressure and the distance from the external boundary to the well. The maximum well capacity without bottom water influx is reached for wells located directly under the reservoir top, i.e., at $H = 0$. In the example considered, for such a well in the critical regime, we obtain $Q_* = 1.1085$ and $p_{1*} = -7.2376$.

That considerable increase in the extent of pumping, compared to the value calculated for $H = 0.2$, is due to an increase in both well productivity and well depth. Therefore, for the normal pumping regime, it is reasonable to lay wells as deep as is possible for the given capacity without water influx, thus minimizing the effect of gravity. For example, if $Q = 0.1$, the normal pumping regime is preserved up to the value $H = 0.7978$, for which $p_1 = -0.6339$, whereas for $H = 0$, we have $p_1 = -1.5559$.

For fixed pressure on the well and the external boundary, the distance L_1 between them is one of the main parameters determining the flow rate. Thus, for $H = 0.2$ and $p_1 = -4$, as L_1 increases from 3 to 7, the capacity Q decreases from 0.7510 to 0.3877. In this case, water spreads over the reservoir bottom: $H_1 = 0.0981$ and 0.1322, $L = 0.0627$ and 0.1776, respectively. We note that, even for $L_1 = 3$, the equipotential is taken to be the external boundary is almost vertical: it reaches the reservoir top at the point with the abscissa $x = 3.00008$.

Another characteristic to be determined is the maximum filtration velocity on the boundary of the flow domain $|w_F|$ and the abscissa x_F of the point F at which this velocity is reached. According to calculations, the point F is on the top or bottom for the well operating at the top or bottom of the reservoir, respectively, and its position is almost independent of the well pressure, whereas the dependence $|w_F|(Q)$ is nearly proportional. For the chosen input parameters over the entire range of the well pressure, $x_F = 0.215$ and $|w_F|/Q = 1.70$ (differences are observed only in the next decimal places).

The parameter ρ has a significant effect on the volume V of the bottom fluid that remains motionless during well pumping; for real values of the parameter ρ are estimated at a few hundredth, the quantities H_1 and L are approximately proportional to this parameter and the quantity V is approximately proportional to its square.

However, the main structural characteristics of the flow are little affected by changes of ρ.

In support of the aforesaid, we give the results of calculations for $H = 0.2$, $\delta = 0.01$, $Q = 1$, $L_1 = 3$, and $\rho = 0.2500$, 0.0250, and 0.0025. For these values of the parameter ρ for the critical flow regime, we have $H_1 = 0.17288$, 0.01776, and 0.00177, $L = 0.113\,064$, 0.011306, and 0.001131, and $V = 66 \cdot 10^{-4}$, $67 \cdot 10^{-6}$, and $67 \cdot 10^{-8}$, respectively; at the same time, for all three versions, we obtained the values $p_1 = -5.062$, $x_F = 0.2146$, and $w_F = -1.701$. The same regularities are also observed for great well depths. In particular, for $H = 0.8$ and the three values of ρ indicated above (the remaining input parameters being the same), we have $V = 74 \cdot 10^{-6}$, $75 \cdot 10^{-8}$, and $75 \cdot 10^{-10}$, $H_1 = 0.018622$, 0.001875, and 0.000187, $L = 0.011936$, 0.001194, and 0.000119, $p_1 = -4.469$, $x_F = 0.2146$, and $w_F = -1.701$, respectively. We note that, in both series (for $h = 0.2$ and 0.8), the values of x_F and w_F are identical, and the only difference is that, in the first series, the point F is at the top of the reservoir, and in the second series, it is at its bottom.

The invariance (noted in Sec. 2) of the geometrical characteristics of the flow under changes in the quantities Q and ρ with the retention of their ratio is also true for the general case, and the filtration velocity components at each point change, as in the critical regime, in proportion to the indicated quantities.

In the case $H = 0$, where the drain A located at the reservoir bottom, is coincident with the corner point E, we have $a = -\infty$. In this case, the relations obtained above and the computational algorithms based on them become much simpler. In particular, for the critical regime, the equality $L \approx \rho/(2Q)$ holds with high accuracy. A nearly linear dependence $L(\rho)$ for the general case was obtained in the example of numerical calculations given above.

We now assume that a heavier fluid is filtered. According to (31) for the former values $\rho_1 = 0.8$ and $\rho_2 = 1$, we have $\rho = 0.2$. The quantity H is the distance from the reservoir bottom to the drain A (see Fig. 6). All details of the analysis performed above are extended to this situation taking into account the reorientation of the flow domain relative to the reservoir top and bottom noted in Sec. 5. In particular, for $H = 0.2$ and $Q = 1$ for the critical regime which is the initial one in the calculations, we have $V = 0.00422$, $p_1 = -5.0623$, $H_1 = 0.1396$, $L = 0.0905$, $x_F = 0.2146$, and $w_F = -1.7013$. A comparison of these values with those obtained for $\rho = 0.25$ confirms the conclusion that the quantity ρ has a significant effect only the parameters of the cone of the quiescent fluid adjacent to the reservoir top in this case. The point F of the maximum filtration velocity is now at the reservoir bottom.

We now consider the case $\rho_1 = 0$, $\rho = 1$ noted in Sec. 5, which is equivalent to fluid filtration in a gas-capped reservoir. In this version for $H = 0.2$ and $Q = 1$ for the critical regime, we obtain $V = 0.0823$, $p_1 = -5.0833$, $H_1 = 0.5180$, $L = 0.4525$, $x_F = 0.2164$, and $w_F = -1.7196$. The volume V of the gas cap that partially penetrates into the reservoir bottom far exceeds the above value found for $\rho_1 = 0.8$. We note that, in this case, the well capacity $Q = 1$ is provided at almost the same pressure p_1 on the well boundary as in the previous calculation version.

Conclusions. Exact solutions of some steady-state problems of fluid influx to a lateral well were constructed for the cases where the reservoir also contains a fluid having different physical parameters and adjacent to the reservoir bottom or top. An algorithm for calculating the auxiliary parameters in the direct formulation was developed. Calculations were performed that allowed a description of the geometrical properties of the flow domain versus well depth, capacity, and pressure. It was shown that the critical flow regime play the determining role in estimating the range of oil reservoir production conditions that rule out the breakthrough of bottom water into the well.

This work was supported by the Russian Foundation for Basic Research (Grant No. 03-05-65299).

REFERENCES

1. P. Ya. Polybarinova-Kochina, *Theory of Motion of Soil Water* [in Russian], Nauka, Moscow (1977).
2. M. Muskat, *The Flow of Homogeneous Fluids through Porous Media*, McGraw Hill, New York (1937).
3. I. A. Charnyi, *Underground Fluid Dynamics* [in Russian], Gostoptekhizdat, Moscow (1963).
4. C. J. Pirson, *Oil Reservoir Engineering,* McGraw-Hill, New York–Toronto–London (1958).
5. R. E. Kidder, "Flow of immiscible fluids in porous media: Exact solution of a free boundary problem," *J. Appl. Phys.*, **17**, No. 8, 867–869 (1956).